

Joint OSNR and Nonlinear Noise Power Estimation Based on Deep Learning for Coherent Optical Communication Systems

Mengyan Li¹, Lifu Zhang¹, Tao Zhang¹, Guozhou Jiang¹, Liu Yang¹, *Member, IEEE*, Fengguang Luo¹, and Yongming Hu¹

Abstract—In this paper, a joint OSNR and nonlinear noise power estimation scheme based on multi-task deep neural network (MT-DNN) is proposed with the advantages of dispersion-insensitive, modulation-format-transparent for high-speed, long-haul, multi-channel fiber-optic communication systems. Amplitude histograms (AHs) are generated by processing the spectrums collected with different OSNR, launch power and transmission distance by an offline spectrum preprocessing flow. The MT-DNN can automatically learn the features of the AHs to achieve OSNR and nonlinear noise power estimation, simultaneously. For 4-quadrature amplitude modulation (4QAM), 16QAM and 64QAM signals under different transmission conditions, the average MAE and RMSE are calculated for the OSNR estimate and the nonlinear noise power estimate, which are both less than 1 dB. Moreover, the resistance of OSNR estimation to amplified spontaneous emission (ASE) noise and nonlinearity, and the tolerance of nonlinear noise estimation to launch power and transmission distance are investigated, respectively. The results demonstrate that the joint OSNR and nonlinear noise power estimation scheme is insensitive to dispersion, transparent to modulation format, and has high accuracy and high tolerance. This research provides a research reference value for future optical performance monitoring of coherent optical communication systems.

Index Terms—Coherent optical communications, optical performance monitoring, optical signal-to-noise ratio, nonlinear noise power, multi-task deep neural networks.

I. INTRODUCTION

IN MULTI-CHANNEL fiber optic communication systems, cross-phase modulation (XPM) is the predominant contribution to nonlinear noise, which can broaden spectrum of

the signal propagating through the fiber [1], [2]. Moreover, in high-speed, long-haul, multi-channel fiber optic communication systems, long-haul transmission and high launch power lead to the accumulation of nonlinearity-induced distortions and the spectrum broadening. In addition, there are interactions between Kerr nonlinearity, chromatic dispersion (CD) and amplified spontaneous emission (ASE) noise from inline amplifiers [3]. These impairments severely limit the capacity and performance of fiber optic communication systems. Optical signal-to-noise ratio (OSNR) and nonlinearity are the most direct and critical factors in measuring the performance of a communication system [4]. Therefore, this requires an intelligent monitoring to estimate OSNR and nonlinear noise power, and thus improves the communication system performance.

To ensure the stable and reliable transmission of fiber optic communication systems, accurate monitoring of OSNR and nonlinearity of fiber optic transmission systems has become a hot research topic, and some related studies have been reported [5], [6], [7], [8], [9], [10], [11], [12], [13], [14], [15], [16], [17], [18], [19], [20], [21]. Traditional OSNR estimation schemes such as error vector magnitude (EVM) [5], amplitude noise correlation function [6] and fractional-order Fourier transform based time domain pilot method [7], etc., have achieved good monitoring performance, but these schemes require a lot of human intervention and will produce inaccurate results if errors occur. With the rapid development of deep learning technology and fiber optic communication systems, deep learning-based OSNR estimation schemes have been proposed [8], [9], [10], which mostly focus on OSNR estimation under single-channel back-to-back transmission or short distance transmission conditions without considering the effect of nonlinear noise. In our previous works, a deep learning-based multi-channel multi-task optical performance monitoring was proposed [11], and then a simplified multi-channel parallel modulation format identification and OSNR estimation based on multi-task deep neural network (MT-DNN) has been proposed [12], but the estimation of nonlinear noise power was not considered. Meanwhile, along with the increasing transmission rate, transmission capacity and transmission distance of fiber optic communication systems, fiber nonlinearity has become the most significant limiting factor and can no longer be ignored. Nonlinear noise power or nonlinear signal-to-noise ratio has been commonly utilized to characterize the effects of fiber nonlinearity [2], [13], [14],

Manuscript received 1 November 2023; accepted 5 November 2023. Date of publication 9 November 2023; date of current version 22 November 2023. This work was supported in part by the National Key R&D Program of China under Grant 2022YFB2903000, in part by the National Natural Science Foundation of China under Grants 62001181 and U21A20500, in part by the Knowledge Innovation Program of Wuhan-Shuguang Project under Grant 202201080102335, and in part by the Natural Science Foundation of Hubei under Grant 2022CFB480. (*Corresponding author: Liu Yang.*)

Mengyan Li, Lifu Zhang, Tao Zhang, Liu Yang, and Yongming Hu are with the School of Microelectronics, Hubei Key Laboratory of Micro-Nanoelectronic Materials and Devices, Hubei University, Wuhan 430062, China (e-mail: liuyang89@hubei.edu.cn).

Guozhou Jiang and Fengguang Luo are with the School of Optical and Electronic Information, Huazhong University of Science and Technology, Wuhan 430074, China, and also with the National Engineering Research Center for Next Generation Internet Access Systems, Wuhan 430074, China.

Digital Object Identifier 10.1109/JPHOT.2023.3331302

[15], [16], [17], [18], [19], [20], [21]. Some nonlinear signal-to-noise ratio estimation schemes based on neural networks have been reported successively [13], [14], [15], [16], [17], [18], [19]. In [15], [17], [19], time-consuming and complex human calculations are required for nonlinear signal-to-noise ratio estimation, such as calculating the phase noise correlation, amplitude noise covariance and second moment statistics of the received signal, etc. In [20], we have proposed an efficient joint nonlinear noise power estimation, OSNR estimation and modulation format identification scheme based on deep learning. An OSNR and nonlinear noise power estimation simultaneously scheme is proposed in [2] and [21]. The estimation scheme of Reference [21] requires the inclusion of a training sequence for frame synchronization, which introduces some complexity. Furthermore, future optical networks will be towards dynamic and heterogeneous, and adaptable to various modulation formats and bit rates [4]. The existing research on nonlinearity focuses on a particular modulation format and does not take into account the adaptability to other modulation formats. Since the received signal is sensitive to dispersion, these schemes mentioned above are implemented based on the received signal and are therefore sensitive to dispersion. And there are not many schemes for joint OSNR and nonlinear noise power estimation until now. Consequently, an efficiency and low-complexity joint OSNR and nonlinear noise power estimation scheme needs to be proposed to meet the needs of future optical networks.

In this paper, based on our previous works [11], [12], [20], we propose a joint estimation scheme of OSNR and nonlinear noise power based on MT-DNN for high-speed, long-haul, multi-channel fiber optic communication systems. In our work, amplitude histograms (AHs) generated based on optical spectrums are fed to a MT-DNN for training to estimate OSNR and nonlinear noise power simultaneously. The effects of ASE noise and nonlinearity on OSNR estimation, and the effects of different launch power and transmission distance on nonlinear noise power estimation are discussed separately. Since the optical spectrum is insensitive to CD and polarization mode dispersion (PMD) [22], [23], this scheme achieves accurate estimation of OSNR and nonlinear noise power even in fiber optic transmission systems with large cumulative dispersion and modulation format transparency.

II. OPERATION PRINCIPLE

A. Amplitude Histograms Based on Optical Spectrums

The principle of AHs generated based on the optical spectrums is shown in Fig. 1. Since this work is a joint OSNR and nonlinear noise power estimation for a high-speed, high-capacity coherent optical communication system, the collected spectrums need to be processed by the spectrum preprocessing flow with low-complexity. The specific processes are downsampling, filtering, power normalization and amplitude histograms generation, as illustrated in the dashed box in Fig. 1. For the 32Gbaud-4QAM optical network with 0 dBm launch power, 26 dB OSNR and 1800 km transmission distance, the spectrum preprocessing process is shown in Fig. 2. Where Fig. 2(a) is the original spectrum collected, Fig. 2(b) is the spectrum after

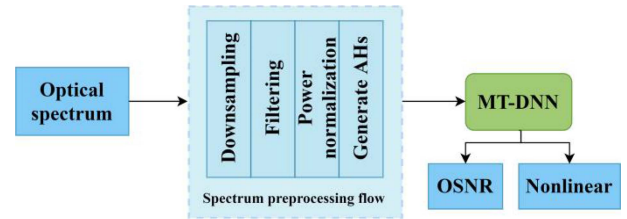


Fig. 1. Schematic of amplitude histograms based on signal spectrums.

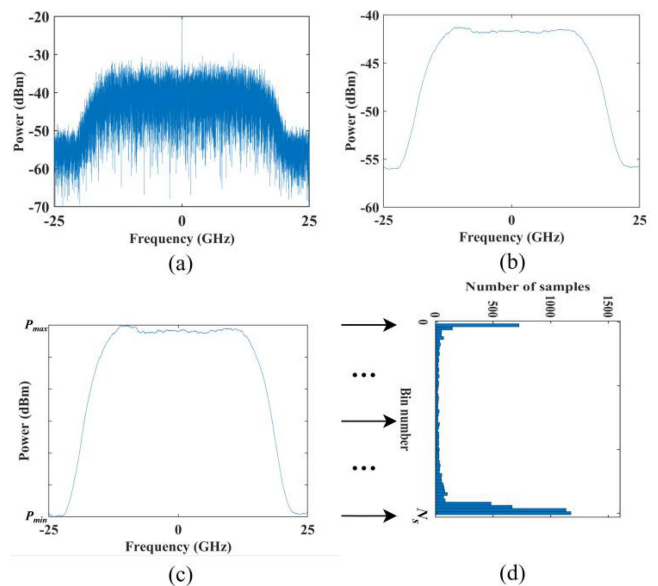


Fig. 2. Process diagram of spectrum preprocessing for 32Gbaud-4QAM optical network.

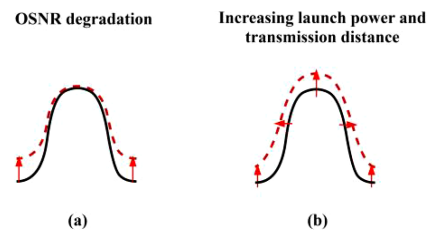


Fig. 3. Optical spectrum variations due to the impairments.

downsampling and filtering process, and Fig. 2(c) is the spectrum power normalization process. To obtain the AHs efficiently and conveniently, we normalize the power in Fig. 2(b). Here we normalize the power to the $[P_{\min}, P_{\max}]$ interval, and then divide the $[P_{\min}, P_{\max}]$ interval equivalently into N_s sub-intervals (here N_s is 60), and finally count the number of signal samples within each sub-interval to generate AHs, as shown in Fig. 2(d). The OSNR degradation caused by the accumulated ASE noise makes the lower part of the optical spectrum submerge below the noise pedestal, and meanwhile raising both of the optical spectrum edges is shown in Fig. 3(a) [22], [24]. From Fig. 3(b), it can be seen that the accumulation of nonlinear noise due to the increasing launch power and transmission distance leads to spectrum broadening and an overall upward shift of the spectrum

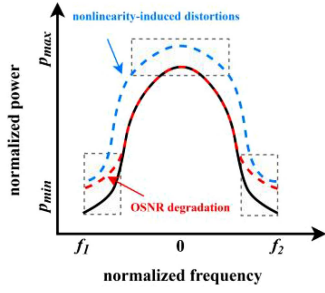


Fig. 4. Linear and nonlinear effects on the optical spectrum.

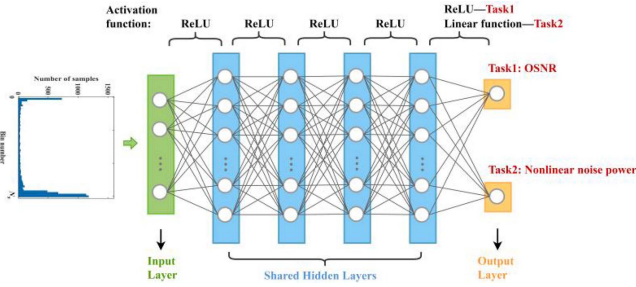


Fig. 5. Structure diagram of MT-DNN used in this paper.

[25]. When the shape of the spectrum changes, we focus on the powers variations to set up the AH to realize the joint estimation of OSNR and nonlinear noise power with the aim of reducing the complexity. When the spectrum is subjected to linear and nonlinear effects, the variations are mainly reflected in the three dashed box parts of Fig. 4. The generated AHs can reflect the statistical distribution of the signal [26]. For 4QAM, 16QAM and 64QAM signals, the corresponding AHs reflect different distribution characteristics at different OSNR, launch power and transmission distance, which will be automatically learned by MT-DNN for joint estimation of OSNR and nonlinear noise power.

B. MT-DNN Principle

Our proposed scheme can achieve the joint estimation of OSNR and nonlinear noise power with the help of MT-DNN. The structure of MT-DNN is shown in Fig. 5 below, which contains 1 input layer, 4 hidden layers and 1 output layer, and the number of nodes contained in each layer is 60, 256, 128, 64, 32, 1/1 in order. The generated AHs are taken as input of MT-DNN, and the output layer containing two tasks, OSNR estimation and nonlinear noise power estimation, are both considered as regression analysis problems. For these two tasks, the hidden layers of MT-DNN share the same mapping, such as the shared hidden layers. The activation functions between the last hidden layer and the output layer are chosen as Rectified Linear Units (ReLU) and linear function for OSNR estimation and nonlinear estimation, respectively. The activation functions between the remaining layers are ReLU function. As for joint OSNR and nonlinear noise power estimation, we assign a loss weight of 1/2 for the OSNR estimation output and the nonlinear noise power

estimation output separately to ensure that they are equally important during MT-DNN training. The mean square error (MSE) function is selected as the loss function. The loss function L of MT-DNN is shown in (1), where MSE_1 and MSE_2 are loss functions of OSNR estimation and nonlinear noise power estimation respectively. MSE_1 and MSE_2 can be expressed by (2), where y_i is the true output, \hat{y}_i is the predicted output of MT-DNN, and m represents the total number of spectrum samples. In addition, mean absolute error (MAE) and root mean square error (RMSE) are adopted as evaluation metrics in the training phase and testing phase of MT-DNN.

$$L = \frac{1}{2} (MSE_1 + MSE_2) \quad (1)$$

$$MSE_1 = MSE_2 = \frac{1}{m} \sum_{i=1}^m (y_i - \hat{y}_i)^2 \quad (2)$$

III. SYSTEM SETUP AND RESULTS

A. System Setup

We set up a high-speed, long-haul, multi-channel coherent optical communication system based on VPI transmission Maker 9.9 and MATLAB. The schematic diagram of MT-DNN based joint OSNR and nonlinear noise power estimation for 3-channel fiber optic communication system is shown in Fig. 6, and the key parameters of this system are shown in Table I. The symbol rate per channel is 32 Gbaud, the channel spacing is 50 GHz, and the center channel is the channel under test. Three widely used signals 4QAM, 16QAM and 64QAM are modulated by a pseudo-random binary sequence (PRBS) of length 2^{15} . The modulated signal is amplified by an erbium-doped fiber amplifier (EDFA), and the launch power is adjusted by a variable optical attenuator (VOA) before being sent into a fiber optic link for transmission. Each span consists of a standard single-mode fiber (SSMF) and an EDFA. At the receiver end, the optical signal is filtered with a 50 GHz bandwidth optical bandpass filter (OBPF) and then coherent detection is conducted.

The joint estimation scheme consists of two stages. In the first stage, the reference value of nonlinear noise power is obtained by simulating a 3-channel coherent optical transmission system with and without nonlinearity, where ASE noise and laser linewidth are not considered. In the second stage, nonlinearity and ASE noise are considered here, and a series of simulations are performed for a 3-channel coherent optical transmission system to obtain reference values of OSNR and spectrum data under different transmission conditions. The reference values of nonlinear noise power are obtained after coherent receiver in electrical domain. The joint estimation of OSNR and nonlinear noise power acquires spectrum data by a optical spectrum analyzer (OSA) in optical domain for the MT-DNN. For 4QAM, 16QAM and 64QAM, 10 sets of data are acquired for each transmission condition considering different OSNR, launch power and transmission distance, with a total of 3780 sets of data acquired. The acquired spectrum data are processed by a spectrum preprocessing flow. Then the generated AHs is randomly divided into training and testing sets in the

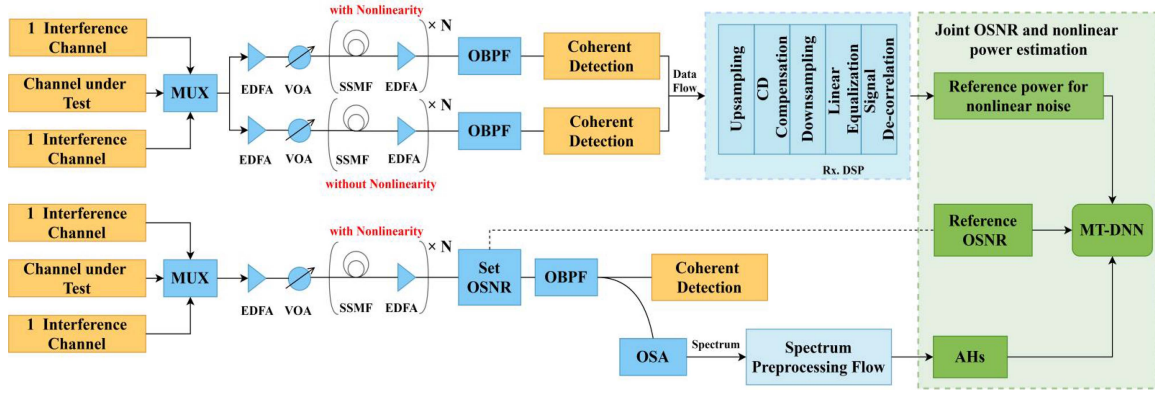


Fig. 6. Schematic diagram of MT-DNN based joint OSNR and nonlinear noise power estimation for 3-channel fiber optic communication system. MUX: Multiplexer; N: Number of fiber spans; Rx.: Receiver; DSP: Digital signal processing.

TABLE I
KEY PARAMETERS OF THE 3-CHANNEL FIBER OPTIC COMMUNICATION SYSTEM

Parameter		Value
Modulation format		4QAM/16QAM/64QAM
Symbol rate		32 Gbaud
SSMF	Length	100 km
	Attenuation	0.2×10^{-3} dB/m
	CD	16×10^{-6} s/m ²
	PMD Coefficient	$0.1 \times 10^{-12}/31.62$ s/(m ^{1/2})
	nonlinear noise refractive index	2.6×10^{-20} m ² /W
Set OSNR	4QAM	16-26 dB (~2dB)
	16QAM	20-30 dB (~2dB)
	64QAM	26-36 dB (~2dB)
Launch power		0-6 dBm (~1dBm)
Transmission distance		600-1800 km (~600km)
Center frequency of the channel under test		193.1 THz
Channel spacing		50 GHz

ratio of 8:2. MT-DNN is built from the Keras library combined with the TensorFlow deep learning framework. Adam optimizer is added to the MT-DNN training phase, and dropout and L2 regularization are used to prevent overfitting [27].

B. Results and Discussion

According to the above scheme, the MT-DNN is trained on the training set, and the performance curves during the training process are shown in Fig. 7. Obviously, the loss of OSNR estimation, nonlinear noise power estimation, and joint OSNR and nonlinear noise power estimation decreases with the increase of training epoch, and finally reaches convergence. In the Fig. 7(b), the average MAE and RMSE of OSNR estimation and nonlinear noise power estimation both gradually decrease with the increase of training epoch, and when the epoch reaches 200, their MAE and RMSE both drop to below 0.30 dB.

The MT-DNN with the scheme doing separate OSNR or nonlinear noise power estimation with a single-task deep neural network (ST-DNN) is compared. The ST-DNN has the same layer structure as the MT-DNN, except for the output layer. The variation curve of error with epoch for ST-DNN (OSNR or nonlinear noise power estimation) is shown in Fig. 8. It can be clearly noticed that the error of separated OSNR or nonlinear noise power estimation is significantly larger than that of OSNR and nonlinear noise power estimation simultaneously. And the error of separated OSNR or nonlinear noise power estimation decreases with increasing epoch and then tends to jitter up and down. This can be explained by the fact that for 4QAM, 16QAM, and 64QAM signals, their OSNR and nonlinear noise power exist the same or close cross values, which is difficult to learn for ST-DNN. As for MT-DNN, the two tasks share the hidden layers, which not only conserves compute resources, but also discovers the connection between the two tasks to improve the estimation performance of MT-DNN. Moreover, the estimation errors of

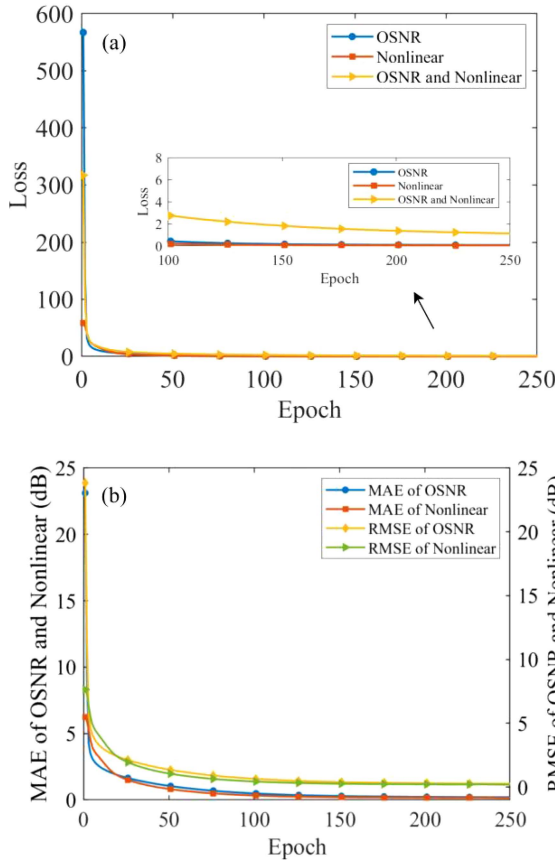


Fig. 7. For joint estimation of OSNR and nonlinear noise power, (a) the variation curve of loss with epoch, (b) the variation curve of error with epoch.

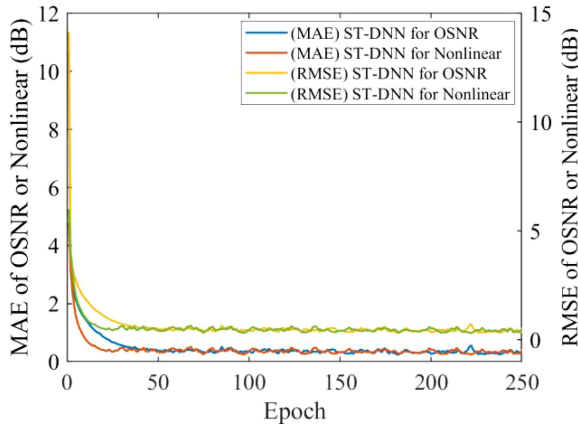


Fig. 8. Variation curve of error with epoch for ST-DNN.

ST-DNN and MT-DNN are shown in Table II. Therefore, we chose to feed the three mixed signals into MT-DNN to estimate OSNR and nonlinear noise power simultaneously.

Based on the trained MT-DNN, the results of OSNR estimation for 4QAM, 16QAM and 64QAM signals are shown in Fig. 9. Fig. 9(a), (b) and (c) show the OSNR estimation errors for the three modulated signals with different launch power and transmission distance, respectively. It can be seen that the higher

TABLE II
COMPARISON OF ESTIMATION ACCURACY

Type of network	Estimation accuracy	
	OSNR (dB)	Nonlinear noise power (dB)
MT-DNN	MAE = 0.26 RMSE = 0.35	MAE = 0.21 RMSE = 0.29
ST-DNN for OSNR	MAE = 0.47 RMSE = 0.74	
ST-DNN for nonlinear		MAE = 0.65 RMSE = 1.10

the order of the modulation format, the larger the OSNR estimation error. This is because that nonlinearity-induced distortion mainly manifests as crosstalk between transmission symbols, and the higher-order modulation format suffers more severely from such crosstalk [28]. The MAE for the three modulated signals can be calculated as 0.21 dB, 0.22 dB and 0.35 dB, respectively. To investigate the resistance of OSNR estimation to different OSNR, we calculated the MAE and RMSE of OSNR estimation for the three modulated signals, as shown in Fig. 9(d). The OSNR estimation errors of the three modulated signals have a roughly increasing trend with increasing OSNR. This can be explained by the fact that when the OSNR is larger, the ASE noise is smaller and the fiber nonlinearity becomes the most significant constraint. In general, the OSNR estimation is accurate even in transmission systems with large cumulative dispersion and nonlinearity. And it is independent of modulation format information, thus this estimation scheme is feasible and robust.

Fig. 10 shows the results of nonlinear noise power estimation for a 16QAM fiber optic transmission system with 1200 km transmission distance. The launch power per channel is from 0 to 6 dBm. It is obvious that the absolute error of the nonlinear noise power estimation varies slightly when OSNR from 20 to 30 dB, and they are all within 0.6 dB. For different OSNR, the estimated nonlinear noise power does not show considerable difference compared to the reference nonlinear noise power. This can also indicate that this nonlinear noise power estimation scheme is not significantly affected by ASE noise.

The accuracy of nonlinear noise power estimation and tolerance to transmission distance and launch power are further investigated. The launch power ranges from 0 to 6 dBm and the transmission distance ranges from 600 to 1800 km. It can be illustrated from Fig. 11 that the reference nonlinear noise power changes correspondingly for the three modulated signals when the launch power and transmission distance vary. It just demonstrates that nonlinear noise is intimately related to launch power and transmission distance [1], [15]. The nonlinear noise power estimation and its error are shown in Fig. 11(a), (b) and (c), and the maximum absolute error is less than 1.0 dB for 4QAM, 16QAM and 64QAM transmission system. There is not a noticeable linear trend in the error of nonlinear noise power estimation when the launch power is from 0 to 6 dBm. However,

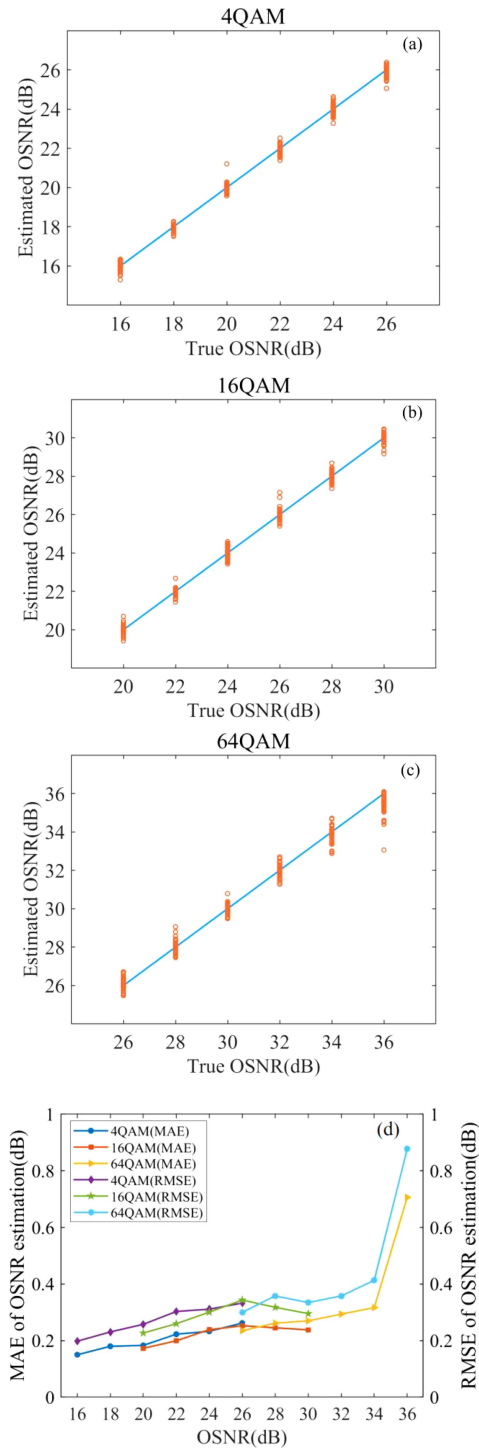


Fig. 9. Based on the trained MT-DNN, (a) estimation error of 4QAM signal, (b) estimation error of 16QAM signal, (c) estimation error of 64QAM signal, (d) MAE and RMSE of OSNR estimation for 4QAM, 16QAM and 64QAM signals.

as a whole, the average error of nonlinear noise power estimation is larger for smaller transmission distances. The reason can be explained by the fact that when the nonlinear noise power is smaller, the effect of nonlinear noise on spectrum is smaller and difficult to be learned by MT-DNN. The MAE of nonlinear noise power estimation are 0.18 dB, 0.20 dB and 0.24 dB for

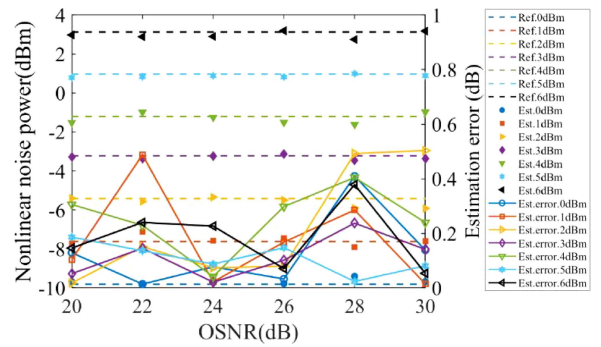


Fig. 10. Nonlinear noise power and its estimation error under different OSNR for a transmission distance of 1200 km with 16 QAM signal.

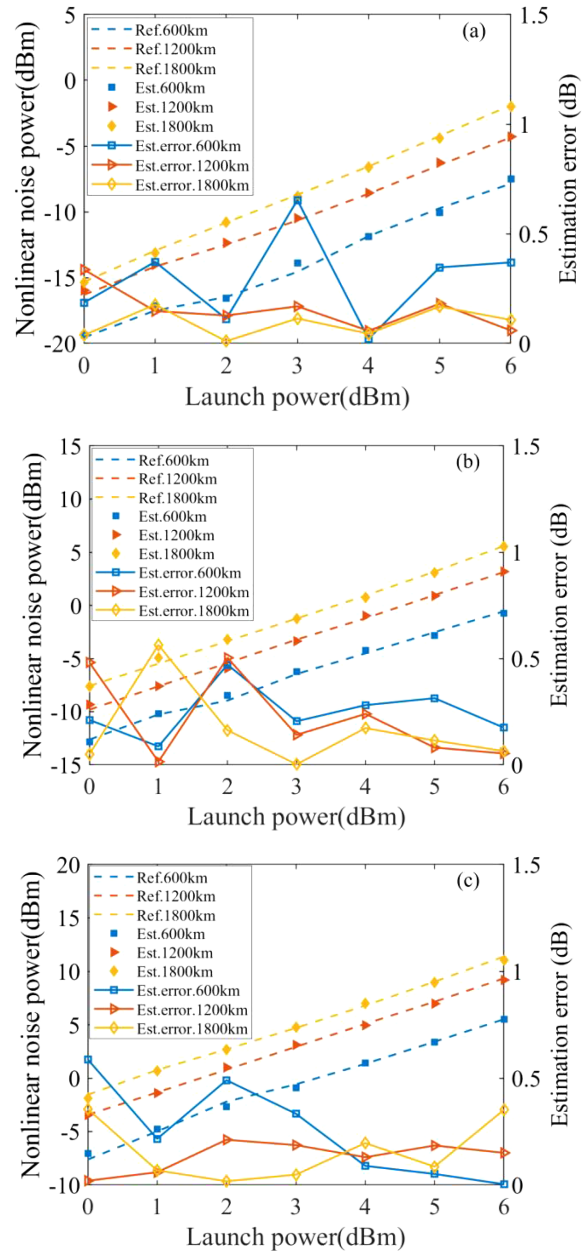


Fig. 11. Estimated nonlinear noise power and its error with different launch power and transmission distance for (a) 4QAM, (b) 16QAM, (c) 64QAM.

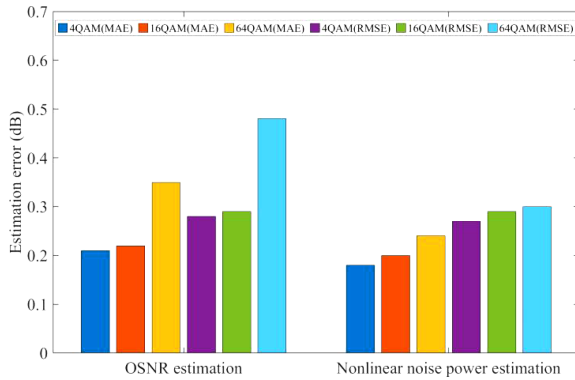


Fig. 12. Overall OSNR and nonlinear noise power estimation error for 4QAM, 16QAM and 64QAM signals.

4QAM, 16QAM and 64QAM signals, respectively. Therefore, the nonlinear noise estimation scheme is precise and tolerant to transmission distance and launch power.

Finally, the errors of OSNR estimation and nonlinear noise power estimation are calculated on all test data for the three modulated signals, as shown in Fig. 12. It can be concluded that the estimation error is larger when the modulation order of the signal is higher, and yet the error is less than 1 dB. This can be explained by the reason that the higher-order modulated signal is more susceptible to nonlinear noise compared to the lower-order modulated signal. For the three modulated signals, the average MAE and RMSE of OSNR estimation are 0.26 dB and 0.35 dB, respectively, and the average MAE and RMSE of nonlinear noise power estimation are 0.21 dB and 0.29 dB, respectively. The proposed joint OSNR and nonlinear noise power estimation scheme is insensitive to dispersion and transparent to modulation format, and with high accuracy and tolerance.

IV. CONCLUSION

In this paper, a MT-DNN-based joint OSNR and nonlinear noise power estimation scheme is proposed, which does not require additional equipment but only an OSA to acquire spectrum. And this processing of spectrum is low complexity and easy to implement. 4QAM, 16QAM and 64QAM modulation formats are investigated under different OSNR, launch power and transmission distance. For OSNR estimation, the estimation error is less than 1.0 dB and is tolerant to ASE noise and nonlinearity. For nonlinear noise power estimation, the estimation error is also less than 1.0 dB and is tolerant for different launch power and transmission distance. The results indicate that this joint estimation scheme is transparent for modulation format information and is insensitive to CD and PMD [22], [23]. The proposed joint OSNR and nonlinear noise power estimation scheme may provide an ideal candidate for future dynamic and flexible optical networks due to the advantages of low complexity and easy implementation.

REFERENCES

[1] G. P. Agrawal, *Nonlinear Fiber Optics*, 5nd ed. New York, NY, USA: Academic, 2013, pp. 258–263.

[2] Z. Wang, A. Yang, P. Guo, and P. He, “OSNR and nonlinear noise power estimation for optical fiber communication systems using LSTM based deep learning technique,” *Opt. Exp.*, vol. 26, pp. 21346–21357, Aug. 2018, doi: [10.1364/OE.26.021346](https://doi.org/10.1364/OE.26.021346).

[3] Q. Fan, G. Zhou, T. Gui, C. Lu, and A. P. T. Lau, “Advancing theoretical understanding and practical performance of signal processing for nonlinear optical communications through machine learning,” *Nature Commun.*, vol. 11, Jul. 2020, Art. no. 3694, doi: [10.1038/s41467-020-17516-7](https://doi.org/10.1038/s41467-020-17516-7).

[4] Z. Dong, F. N. Khan, Q. Sui, K. Zhong, C. Lu, and A. P. T. Lau, “Optical performance monitoring: A review of current and future technologies,” *J. Lightw. Technol.*, vol. 34, no. 2, pp. 525–543, Jan. 2016, doi: [10.1109/JLT.2015.2480798](https://doi.org/10.1109/JLT.2015.2480798).

[5] R. Schmogrow et al., “Error vector magnitude as a performance measure for advanced modulation formats,” *IEEE Photon. Technol. Lett.*, vol. 24, no. 1, pp. 61–63, Jan. 2012, doi: [10.1109/LPT.2011.2172405](https://doi.org/10.1109/LPT.2011.2172405).

[6] Z. Wang, A. Yang, P. Guo, Y. Lu, and Y. Qiao, “Nonlinearity-tolerant OSNR estimation method based on correlation function and statistical moments,” *Opt. Fiber Technol.*, vol. 39, pp. 5–11, Dec. 2017, doi: [10.1016/j.yofte.2017.09.016](https://doi.org/10.1016/j.yofte.2017.09.016).

[7] W. Wang, A. Yang, P. Guo, Y. Lu, and Y. Qiao, “Joint OSNR and interchannel nonlinearity estimation method based on fractional Fourier transform,” *J. Lightw. Technol.*, vol. 35, no. 20, pp. 4497–4506, Oct. 2017, doi: [10.1109/JLT.2017.2744666](https://doi.org/10.1109/JLT.2017.2744666).

[8] D. Wang et al., “Intelligent constellation diagram analyzer using convolutional neural network-based deep learning,” *Opt. Exp.*, vol. 25, no. 15, pp. 17150–17166, Jul. 2017, doi: [10.1364/OE.25.017150](https://doi.org/10.1364/OE.25.017150).

[9] H. Lu et al., “OSNR monitoring using mean and variance values of signal amplitude combination with DNNs,” in *Proc. IEEE 14th Int. Conf. Adv. Infocomm Technol.*, 2022, pp. 90–93.

[10] C. Wang, S. Fu, Z. Xiao, M. Tang, and D. Liu, “Long short-term memory neural network (LSTM-NN) enabled accurate optical signal-to-noise ratio (OSNR) monitoring,” *J. Lightw. Technol.*, vol. 37, no. 16, pp. 4140–4146, Aug. 2019, doi: [10.1109/JLT.2019.2904263](https://doi.org/10.1109/JLT.2019.2904263).

[11] S. Yang et al., “Multi-channel multi-task optical performance monitoring based multi-input multi-output deep learning and transfer learning for SDM,” *Opt. Commun.*, vol. 495, Sep. 2021, Art. no. 127110, doi: [10.1016/j.optcom.2021.127110](https://doi.org/10.1016/j.optcom.2021.127110).

[12] M. Li et al., “Simplified multi-channel parallel optical performance monitoring based on deep learning,” *Acta Optica Sinica*, vol. 43, no. 7, Jan. 2023, Art. no. 0715002, doi: [10.3788/AOS222033](https://doi.org/10.3788/AOS222033).

[13] A. S. Kashi et al., “Nonlinear signal-to-noise ratio estimation in coherent optical fiber transmission systems using artificial neural networks,” *J. Lightw. Technol.*, vol. 36, no. 23, pp. 5424–5431, Dec. 2018, doi: [10.1109/JLT.2018.2873949](https://doi.org/10.1109/JLT.2018.2873949).

[14] M. Al-Nahhal, I. Al-Nahhal, O. A. Dobre, X. Lin, D. Chang, and C. Li, “Joint estimation of linear and nonlinear coherent optical fiber signal-to-noise ratio,” *IEEE Photon. Technol. Lett.*, vol. 35, no. 1, pp. 23–26, Jan. 2023, doi: [10.1109/LPT.2022.3218611](https://doi.org/10.1109/LPT.2022.3218611).

[15] F. J. Vaquero Caballero et al., “Machine learning based linear and nonlinear noise estimation,” *J. Opt. Commun. Netw.*, vol. 10, no. 10, pp. D42–D51, Jun. 2018, doi: [10.1364/JOCN.10.000D42](https://doi.org/10.1364/JOCN.10.000D42).

[16] M. Al-Nahhal, I. Al-Nahhal, O. A. Dobre, S. K. O. Soman, D. Chang, and C. Li, “Learned signal-to-noise ratio estimation in optical fiber communication links,” *IEEE Photon. J.*, vol. 14, no. 6, Dec. 2022, Art. no. 7260107, doi: [10.1109/JPHOT.2022.3222264](https://doi.org/10.1109/JPHOT.2022.3222264).

[17] X. Liu, H. Lun, M. Fu, L. Yi, W. Hu, and Q. Zhuge, “Machine learning based fiber nonlinear noise monitoring for subcarrier-multiplexing systems,” in *Proc. Opt. Fiber Commun. Conf. Exhib.*, 2020, pp. 1–3.

[18] A. S. Kashi, J. C. Cartledge, and W.-Y. Chan, “Neural network training framework for nonlinear signal-to-noise ratio estimation in heterogeneous optical networks,” in *Proc. Opt. Fiber Commun. Conf. Exhib.*, 2021, pp. 1–3.

[19] A. S. Kashi et al., “Fiber nonlinear noise-to-signal ratio monitoring using artificial neural networks,” in *Proc. Eur. Conf. Opt. Commun.*, 2017, pp. 1–3.

[20] S. Yang et al., “Joint fiber nonlinear noise estimation, OSNR estimation and modulation format identification based on asynchronous complex histograms and deep learning for digital coherent receivers,” *Sensors*, vol. 21, no. 2, Jan. 2021, Art. no. 380, doi: [10.3390/s21020380](https://doi.org/10.3390/s21020380).

[21] Y. Xiang et al., “A joint OSNR and nonlinear distortions estimation method for optical fiber transmission system,” *IEEE Photon. J.*, vol. 10, no. 5, Oct. 2018, Art. no. 7907811, doi: [10.1109/JPHOT.2018.2873778](https://doi.org/10.1109/JPHOT.2018.2873778).

[22] H. Wang, S. Cui, C. Ke, C. Yu, Z. Liang, and D. Liu, “Multi-functional optical spectrum analysis using multi-task cascaded neural networks,” *IEEE Photon. J.*, vol. 14, no. 4, Aug. 2022, Art. no. 7241609, doi: [10.1109/JPHOT.2022.3187648](https://doi.org/10.1109/JPHOT.2022.3187648).

- [23] H. Zheng et al., "Modulation format-independent optical performance monitoring technique insensitive to chromatic dispersion and polarization mode dispersion using a multi-task artificial neural network," *Opt. Exp.*, vol. 28, no. 22, pp. 32331–32341, Oct. 2020, doi: [10.1364/OE.402939](https://doi.org/10.1364/OE.402939).
- [24] L. Shu, Z. Yu, Z. Wan, J. Zhang, S. Hu, and K. Xu, "Dual-stage soft failure detection and identification for low-margin elastic optical network by exploiting digital spectrum information," *J. Lightw. Technol.*, vol. 38, no. 9, pp. 2669–2279, May 2020, doi: [10.1109/JLT.2019.2947562](https://doi.org/10.1109/JLT.2019.2947562).
- [25] C. Yu, H. Wang, C. Ke, Z. Liang, S. Cui, and D. Liu, "Multi-task learning convolutional neural network and optical spectrums enabled optical performance monitoring," *IEEE Photon. J.*, vol. 14, no. 2, Apr. 2022, Art. no. 7217808, doi: [10.1109/JPHOT.2022.3153638](https://doi.org/10.1109/JPHOT.2022.3153638).
- [26] Y. Cheng, S. Fu, M. Tang, and D. Liu, "Multi-task deep neural network (MT-DNN) enabled optical performance monitoring from directly detected PDM-QAM signals," *Opt. Exp.*, vol. 27, no. 13, pp. 19062–19074, Jun. 2019, doi: [10.1364/OE.27.019062](https://doi.org/10.1364/OE.27.019062).
- [27] D. Soydaner, "A comparison of optimization algorithms for deep learning," *Int. J. Pattern Recognit. Artif. Intell.*, vol. 34, no. 13, Apr. 2020, Art. no. 2052013, doi: [10.1142/S0218001420520138](https://doi.org/10.1142/S0218001420520138).
- [28] A. Amari, O. A. Dobre, R. Venkatesan, O. S. S. Kumar, P. Ciblat, and Y. Jaouën, "A survey on fiber nonlinearity compensation for 400 Gb/s and beyond optical communication systems," *IEEE Commun. Surveys Tuts.*, vol. 19, no. 4, pp. 3097–3113, Fourthquarter 2017, doi: [10.1109/COMST.2017.2719958](https://doi.org/10.1109/COMST.2017.2719958).